Utilizing Moment Tensors to Characterize Out-of-Zone Steam Chamber Growth

Ted Urbancic, Katherine Buckingham, Anisa Kassam, and Adam Baig, Engineering Seismology Group, Kingston, Ontario, Canada; Said Mahrooqi, Forbes Clow, and Said Busaidi, Petroleum Development Oman*

Summary

Microseismic monitoring has long been used to monitor steam injection programs related to enhanced heavy oil recovery. It has been well established that microseismicity can be used to examine steam chamber dimensions, cap rock integrity or steam containment and fault activation associated with injections. More recently, source parameter investigations have identified the stress transfer mechanism associated with steam chamber development and the re-distribution of stress to allow for out-of-zone growth. The underlying process associated with out-of-zone growth, however, has remained elusive. Here, we consider seismicity associated with a steam injection into an oil bearing reservoir in North Oman. Utilizing a multi-well multi-array configuration, moment tensor inversion was carried out for 824 microseismic events (571 general solutions, 253 double couple solutions) occurring both in the reservoir formation as well as in the adjoining cap rock. Our analysis showed a progressive change in principal stress-strain axes with decreasing depth, suggesting a flip in magnitude occurs between the reservoir and the cap rock thereby allowing for the activation of large structures and out-of-zone growth. Events within the reservoir appear to be dominated by volumetric failures whereas within the cap rock, shear-tensile failures with opening and closure events predominate. Based on these observations, we suggest that moment tensor analysis provides an approach for identifying the underlying processes associated with steam injection and moreover, that local variations in the stress-strain field due to steam injection can result in optimal orientations to allow for the activation of pre-existing faults, in this case located in the cap rock.

Introduction

The monitoring of steam injection programs for well over a decade, be they cyclic steam, Huff and Puff, SAGD, or some combination thereof have been utilizing microseismicity to, for example, track steam movement within the reservoir, identify well casing failures, recognize potential cap rock integrity issues, and characterize the activation of faults. Talebi et. al. (1998) identified that the similar partition between P- and S-wave energy was indicative of well casing failures during CSS operations. A similar observation was made by Urbancic et. al. (2009), where they were able to show a predominantly tensile failure in the region of the cap rock, albeit for a CO2 sequestration experiment. Further investigations by Urbancic et. al. (2010) in both Huff and Puff and CSS operations were able to identify that the reservoir was storing energy that subsequently through a stress transfer mechanism was over time conveyed to the cap rock. McGillvary (2005) showed that the distribution of event locations defined the leading edge of the steam chamber and that the areal coverage in seismicity defined the volumetric extent of the subsequent steam injection. Additional analysis of seismicity associated with steam chamber development, including moment tensor analysis by Baig and Urbancic (2010a) showed how failures within the steam chamber (Huff and Puff injection) were dominated by either volumetric increases or collapse. That behavior was uniquely different from the movement of steam along pre-existing fault/fractures that tended to be shear-tensile failures. In these examples, and in many others, the mechanism for the transition between reservoir and cap rock or reservoir and pre-existing fractures is not well understood. Although the analysis of microseismic events themselves shows the resultant effect, the question is whether microseismicity can be used to provide more details on how and why the transitions occur.

In this study, we analyze seismicity associated with the injection of steam from two injectors into two horizons within a reservoir in North Oman over an approximate two-month period and the subsequent two-month soak cycle. A total of five monitoring wells consisting of a minimum of two to eight three component 15Hz geophones were installed surrounding the volume encompassing the two injectors. As shown in Figure 1, the reservoir is sub-divided into five major units (Upper Reservoir UR1 – UR3, Lower Reservoir LR1 - LR2). During this injection cycle, following initial build-up, steam was injected into the UR1 and LR2 units varying from 200 – 400 tonnes/day. The reservoir is overlain by a formation, which acts as the capping rock for the reservoir. Over the monitoring period a total of 824 events were recorded on multiple arrays and subsequently located utilizing P- and S-wave first arrivals, hodograms and ray-tracing based downhill simplex algorithm. This data set formed the basis for the current study.

In addition to utilizing first arrival data, the waveforms of individual events themselves contain information about the types of failure responsible for the observed signals. Seismic Moment Tensor Inversion (SMTI) analysis, such as described by Baig and Urbancic (2010b) can be utilized to identify the modes of fracturing. The moment tensor is a representation of the failure mechanism that controls the amplitudes and polarities of the waveforms of P, SV, and SH waves that propagate outwards from the event hypocenter. The process of seismic moment tensor

DOI http://dx.doi.org/10.1190/segam2013-1367.1

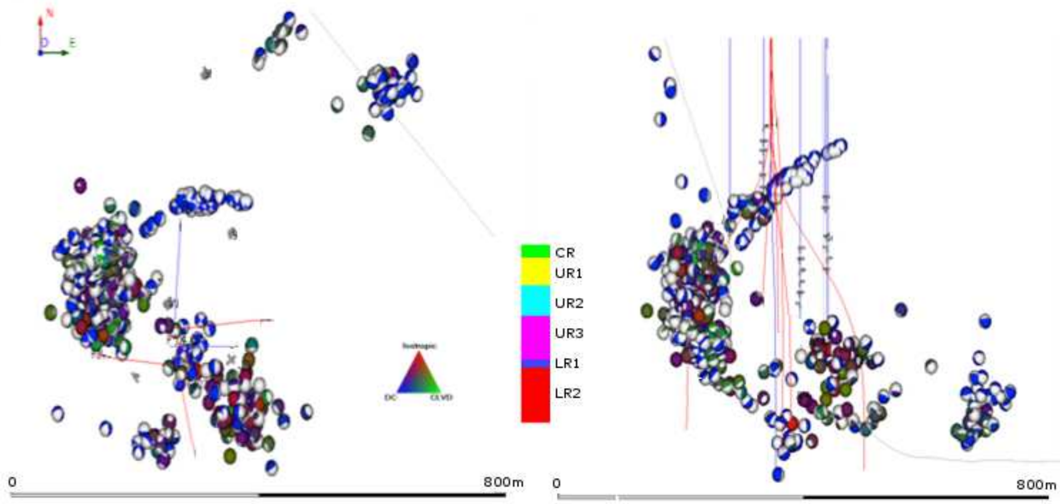

Figure 1. Observed seismicity in plan and depth views. Moment tensor derived mechanisms are plotted based on either General or Double Couple solutions. Injection was in the upper most (UR1) and lowest (LR2) reservoir units. CR is the capping rock.

inversion (SMTI) involves observing these waveforms and projecting the amplitudes back to the hypocenter to determine the mechanism. In order to get a stable solution, the sensors recording the waveforms, as configured for this study, must be deployed in a three-dimensional network around the events. In general, the inversion results can be visualized using source-type diagrams (Hudson et al., 1989) where mechanisms consistent with crack opening or closing, volumetric and pure-shear failures, or mixed-mode failures can be identified (General solutions). Consideration of these different source types can be used to resolve the strain equivalent principal axes of the moment tensor (i.e. pressure, P, intermediate B, and tension, T). Shear dominated events (Double Couple solutions) can be grouped using a nearest neighbor approach and the (best-fitting) local stress field determined and used to define the likely fracture orientations of individual events, similar to the approach described by Gephart and Forsyth, 1984. Similarly, it is considered that fracture planes for failures exhibiting significant opening components of failure are normal to the T axis whereas closure dominated events the fracture are normal to the P axis.

Here, we examine the distribution of moment tensor derived principal strain axes both spatially and temporally for a total of 824 events (571 general solutions, 253 double couple solutions) occurring both in the reservoir formation as well as in the adjoining cap rock. Our analysis will focus on identifying any characteristic changes in principal strain axes and source mechanisms with decreasing depth, between the reservoir and the cap rock. Additionally, we examine the identification and activation of large structures and their potential influence on out-of-zone growth. Based on these observations, we discuss how stress transfer can occur between the reservoir and overlying cap rock, and the underlying processes that may be responsible for the observed behavior.

Analysis

The inversion results for the recorded events are shown in Figure 1 in both plan and depth view. Stereographic projections are plotted at each event location and are color coded by the dominant mode of failure. Most of the events are clustered in the vicinity of the injectors within the reservoir, however, there appears to be both downward growth into the lower reservoir as well as upward growth into the cap rock. Numerous events for these out-of-zone growth regions appear to follow planar trends, suggestive that the observed growth is related to the activation of larger structures.

Within the reservoir, there are numerous events with significant volumetric components of failure, including CLVD (Compensated Linear Vector Dipole) dominated failures related to new fracture development. Event clusters located at distance from the main cluster, although broadly distributed appear to have similar failure plane orientations, also suggestive that larger features are being activated due to stress re-distribution resulting from the injection program.

In general, this process can be suggested for the majority of the events that occurred during the soak cycle, suggesting that the observed activity was related to stress relaxation and the resulting stress transfer process than related to a stress driven process commonly associated with steam injection programs.

DOI http://dx.doi.org/10.1190/segam2013-1367.1

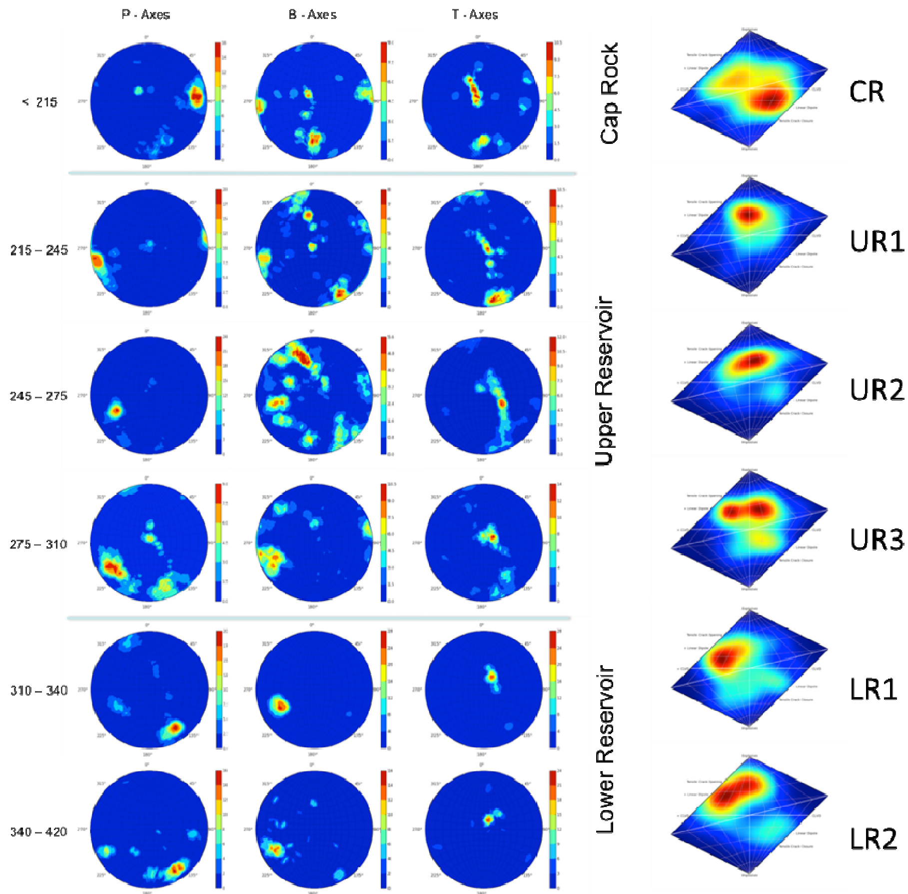

Figure 2: Figure 2: Contoured principal strain axes (P, B, and T) as a function of depth along with their corresponding Hudson k-T plots. Depths are provided in meters.

To examine the stress-strain behavior within the main zone of observed seismicity, the events were separated into five depth intervals within the reservoir and into a single zone above the reservoir into the cap rock. The division of seismicity was strictly based on depth, similarity in spatial event trends, and ensuring there was a representative number events within each grouping to allow for the inversion of the principal stress axes. The lithologic divisions were also used as a guide in the depth interval selection but were not strictly adhered to. In Figure 2, the principal strain axes as a function of depth interval are shown along with their respective Hudson plots. What is striking is the transition in dominant orientations for the P, B, and T axes moving from the lower reservoir to the cap rock at shallower depth. Within the lower reservoir, the principal strain axes appear to be relatively stable, with sub-horizontal P and B axes trending to the southeast and southwest respectively, and with sub-vertical T axes. Within the upper reservoir, corresponding to the injection layers, the maximum strain (P axes) transitions from southeast to southwest at shallower depths. Similarly, the minimum strain begins to transition within the upper reservoir from sub-vertical to a sub-horizontal southeast orientation. This is particularly evident between 245m and 275m. The complexity of the strain field is certainly evident within the upper reservoir, which is likely indicative of steam chamber development. Above the reservoir, there appears generally to be a flip between the maximum and intermediate strain axes as compared to what is observed in the lower reservoir. At both depths, the minimum strain remains predominantly sub-vertical. By further applying an approach similar to that proposed by Gephart and Forsyth (1984), utilizing a nearest neighbors for events within each depth interval, we calculate their average stress axes. The principal stress axes, as shown in Figure 3, are mapped in terms of a stress path, from the lower reservoir to the cap rock. Following the maximum principal stress, three broadly defined stress behaviors are observed corresponding to the lower and upper reservoir, and the cap rock. Based on these observations, we can

DOI http://dx.doi.org/10.1190/segam2013-1367.1

speculate that the transition or rotation in principal stress-strain axes represents a change in the stress-strain magnitudes with depth and is responsible for the activation of pre-existing structures within the cap rock.

In Figure 2 we also show the failure mechanisms on Hudson k-T plots by depth intervals. Within the lower reservoir and in the cap rock, the failures are dominated by shear-tensile failures. This is similar to what is observed in hydraulic fracture stimulations where fluid injection results in the development of a discrete fracture network with mixed-mode failures. Within the upper reservoir, which corresponds to the injection interval, volumetric opening failures dominate and thereby can be directly related to the development and growth of the steam chamber. These observations are very similar to those by Baig and Urbancic (2010a), where they observed volumetric opening and closing events associated with a Huff and Puff steam injection in diatomite within the reservoir and vertical growth shear-tensile failures along a pre-existing fracture set out of the reservoir. Figure 4 identifies the fractures associated with the different depth intervals. Of note is the simplicity of the fracture orientations in the lower reservoir and cap rock as compared to the fractures in the upper reservoir, which represents a complex fracturing pattern as would be expected during steam chamber development.

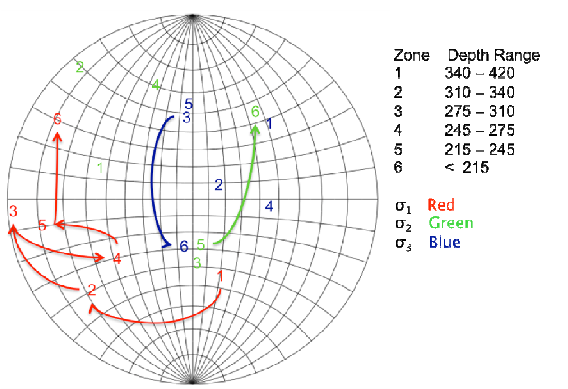

Figure 3. Stereographic projection of the principal stress axes for the depth intervals (1-6). Also shown are the stress paths for the maximum principal stress as well as the transition to cap rock activity for the intermediate and minor stress axes.

Conclusions

In this study we have examined the stress-strain behavior associated with steam chamber growth and the conditions leading up to out-of-zone growth and development. The underlying process appears to be related to the rotation in the principal stresses along a stress path that thereby allows for fracture sets, previously clamped, to be activated resulting in out-of-zone growth. Within the upper reservoir (injection related), the observed behavior is in-line with observations of volumetric steam chamber development reported in the literature. It is also within the upper reservoir that a significant increase in fracture complexity is observed, which is in marked contrast to the singular shear-tensile behavior observed in the cap rock and lower reservoir. Based on these observations, we suggest that moment tensor analysis provides an approach for identifying the underlying processes associated with steam injection and moreover, that local variations in the stress-strain field due to steam injection can result in optimal orientations to allow for the activation of pre-existing faults, in this case located in the cap rock.

Acknowledgments

The authors would like to thank Petroleum Development Oman (PDO) and the Minister of Oil and Gas, Sultanate of Oman, for permission to publish this paper. We also wish to acknowledge, ESG solutions and all PDO geophysicists for the support throughout design, processing and analyses.

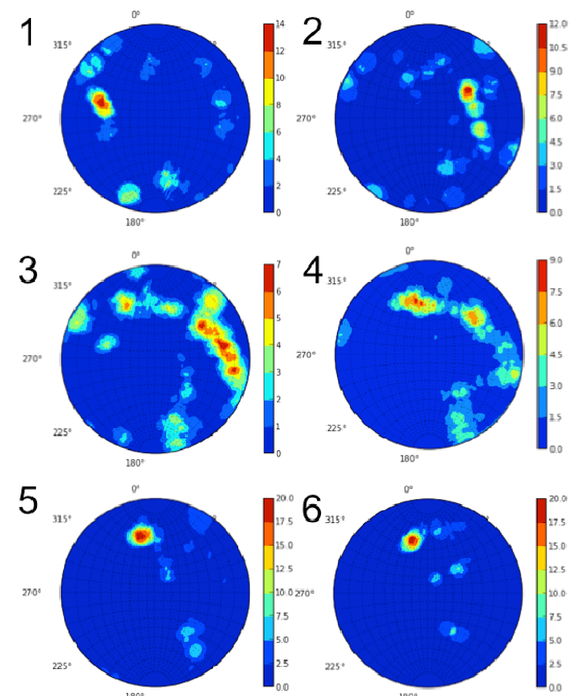

Figure 4. Pole concentrations for the dominant planes in each depth interval using the principal stresses and depth intervals outlined in Figure 3

http://dx.doi.org/10.1190/segam2013-1367.1

EDITED REFERENCES

Note: This reference list is a copy-edited version of the reference list submitted by the author. Reference lists for the 2013 SEG Technical Program Expanded Abstracts have been copy edited so that references provided with the online metadata for each paper will achieve a high degree of linking to cited sources that appear on the Web.

REFERENCES

Baig, A., and T. I. Urbancic, 2010, Microseismic moment tensors: A path to understanding frac growth: The Leading Edge, **29**, 320–324, http://dx.doi.org/10.1190/1.3353729.

Baig, A. M., T. I. Urbancic, and M. Seibel, 2011, Steam chamber development in diatomites: The role of microseismic monitoring in identifying conformance and out-of-zone fracture growth: SPE 147399.

Daugherty, J., and T. Urbancic, 2009, Microseismic monitoring or a carbon sequestration field test: Frontiers + Innovation – 2009 CSPG CSEG CWLS Convention, Abstract Archive, 259–261.

Gephart, J. W., and D. W. Forsyth, 1984, An improved method for determining the regional stress tensor using earthquake focal mechanism data: Application to the San Fernando Earthquake Sequence: Journal of Geophysical Research, **89**, B11, 9305–9320, http://dx.doi.org/10.1029/JB089iB11p09305.

Hudson, J. A., R. G. Pearce, and R. M. Rogers, 1989, Source type plot for inversion of the moment tensor: Journal of Geophysical Research, **94**, B1, 765–774, http://dx.doi.org/10.1029/JB094iB01p00765.

McGillivray, P., 2005, Microseismic and time-lapse seismic monitoring of a heavy oil extraction process at Peace River, Canada: CSEG Recorder, **30**, no. 1, 5–9.

Talebi, S., T. J. Boone, and S. Nechtschein, 1998, A seismic model of casing failure in oil fields: Pure and Applied Geophysics, **153**, no. 1, 197–217, http://dx.doi.org/10.1007/s000240050192.

Urbancic, T., M. Prince, and A. Baig, 2011, Long-term assessment of reservoir integrity utilizing seismic source parameters as recorded with integrated microseismic-pressure arrays: 81st Annual International Meeting, SEG, Expanded Abstracts, 1529–1533.